LUMIO

An Autonomous CubeSat for Lunar Exploration

Speretta, Stefano; Cervone, Angelo; Sundaramoorthy, Prem; Noomen, Ron; Mestry, Samiksha; do Carmo Cipriano, Ana; Topputo, Francesco; Ivanov, Anton; Vennekens, Johan; More Authors

DOI
10.1007/978-3-030-11536-4_6

Publication date
2019

Document Version
Final published version

Published in
Space Operations

Citation (APA)
Speretta, S., Cervone, A., Sundaramoorthy, P., Noomen, R., Mestry, S., do Carmo Cipriano, A., Topputo, F., Ivanov, A., Vennekens, J., & More Authors (2019). LUMIO: An Autonomous CubeSat for Lunar Exploration. In H. Pasquier, C. A. Cruzen, M. Schmidhuber, & Y. H. Lee (Eds.), *Space Operations: Inspiring Humankind's Future* (pp. 103-134). Springer. https://doi.org/10.1007/978-3-030-11536-4_6

LUMIO: An Autonomous CubeSat for Lunar Exploration

Stefano Speretta, Angelo Cervone, Prem Sundaramoorthy, Ron Noomen, Samiksha Mestry, Ana Cipriano, Francesco Topputo, James Biggs, Pierluigi Di Lizia, Mauro Massari, Karthik V. Mani, Diogene A. Dei Tos, Simone Ceccherini, Vittorio Franzese, Anton Ivanov, Demetrio Labate, Leonardo Tommasi, Arnoud Jochemsen, Jānis Gailis, Roberto Furfaro, Vishnu Reddy, Johan Vennekens and Roger Walker

Abstract The Lunar Meteoroid Impact Observer (LUMIO) is one of the four projects selected within ESA's SysNova competition to develop a small satellite for scientific and technology demonstration purposes to be deployed by a mothership around the Moon. The mission utilizes a 12U form-factor CubeSat which carries the LUMIO-Cam, an optical instrument capable of detecting light flashes in the visible spectrum to continuously monitor and process the meteoroids impacts. In this chapter, we will describe the mission concept and focus on the performance of a novel navigation concept using Moon images taken as byproduct of the LUMIO-Cam operations. This new approach will considerably limit the operations burden on ground, aiming at autonomous orbit-attitude navigation and control. Furthermore, an efficient and autonomous strategy for collection, processing, categorization, and storage of payload data is also described to cope with the limited contact time and downlink bandwidth. Since all communications have to go via a lunar orbiter, all commands and telemetry/data will have to be forwarded to/from the mothership. This will prevent quasi-real-time operations and will be the first time for CubeSats

S. Speretta (✉) · A. Cervone · P. Sundaramoorthy · R. Noomen · S. Mestry · A. Cipriano
Delft University of Technology, Delft, The Netherlands
e-mail: s.speretta@tudelft.nl

F. Topputo · J. Biggs · P. Di Lizia · M. Massari · K. V. Mani · D. A. Dei Tos · S. Ceccherini · V. Franzese
Politecnico Di Milano, Milan, Italy

A. Ivanov
Space Center, Skolkovo Institute of Science and Technology, Moscow, Russia

D. Labate · L. Tommasi
Leonardo, Campi Bisenzio, Florence, Italy

A. Jochemsen · J. Gailis
Science and Technology AS, Oslo, Norway

R. Furfaro · V. Reddy
University of Arizona, Tucson, AZ, USA

J. Vennekens · R. Walker
European Space Agency, Noordwijk, The Netherlands

H. Pasquier et al. (eds.), *Space Operations: Inspiring Humankind's Future*,
https://doi.org/10.1007/978-3-030-11536-4_6

as they have never flown without a direct link to Earth. This chapter was derived from a paper the authors delivered at the SpaceOps 2018 conference [1].

Nomenclature

ADCS	Attitude determination and control system
CCD	Charge-coupled device
CCSDS	Consultative committee for space data systems
CDF	Concurrent Design Facility
CONOPS	Concept of operations
COTS	Commercial off the shelf
CRTBP	Circular restricted three-body problem
EOL	End of life
ESA	European Space Agency
FOV	Field of view
HIM	Halo injection maneuver
IMU	Inertial measurement unit
LUCE	Lunar CubeSat for exploration
LUMIO	Lunar Meteoroid Impact Observer
NIR	Near infrared
OBPDP	Onboard payload data processor
PCM	Plane change maneuver
RF	Radio frequency
ROM	Rough order of magnitude
SADA	Solar array drive assembly
SK	Station keeping
SMIM	Stable manifold injection maneuver
SNR	Signal-to-noise ratio
TCM	Trajectory correction maneuver
TRL	Technology readiness level
UHF	Ultra-high frequency

1 Introduction

The Lunar Meteoroid Impact Observer (LUMIO) was one of the proposals submitted to the ESA SysNova LUnar CubeSats for Exploration (LUCE) call by ESA [2]. SysNova is intended to generate new and innovative concepts and to verify quickly their usefulness and feasibility via short concurrent studies. LUMIO was selected as one of the four concurrent studies run by ESA, and it won ex aequo the challenge. An independent assessment conducted at ESA's Concurrent Design Facility (CDF) has

shown that the mission is feasible, proving the value of LUMIO for future autonomous missions for planetary exploration.

The mission utilizes a CubeSat that carries the LUMIO-Cam, an optical instrument capable of detecting light flashes in the visible spectrum. Onboard data processing is implemented to minimize data downlink, while still retaining relevant scientific data. The mission implements a sophisticated orbit design: LUMIO is placed in a halo orbit about Earth–Moon L_2 where permanent full-disk observation of the lunar farside is made. This prevents background noise due to Earthshine and permits obtaining high-quality scientific products.

This chapter will focus on the concept of operations, which will not have a direct communication link to Earth, preventing the usual navigation and control techniques. LUMIO will be especially relevant as a precursor of autonomous missions to remote bodies which cannot rely on real-time commands. Furthermore, in the optics of reducing the cost of a mission, operations (and navigation) will be autonomous, as operations are one of the cost figures that do not scale linearly with satellite size [3].

In this chapter, we will present the mission (Sect. 2), briefly describing also the SysNova LUCE challenge. We will then describe the satellite design (Sect. 3) and the orbit design (Sect. 4) and concentrate on the mission concept of operations (Sect. 5) and the autonomous navigation system (Sect. 6). The concept presented throughout this chapter has also been independently verified by the ESA CDF team (Sect. 7) that suggested improvements to the mission.

2 Mission Description

LUMIO was one of the four competitive proposals selected for the ESA SysNova LUCE [1] study, which was aimed at identifying a viable low-cost concept using nanosatellites or CubeSats for interplanetary exploration. The LUCE call was, in particular, aimed at technology demonstration and the exploration of the Moon. The prize for this competitive study was the opportunity to review and advance the mission concept with ESA experts at the CDF at ESA/ESTEC. This independent mission verification was carried out and showed that the mission is feasible and suggested a series of improvements, described in Sect. 7.

2.1 SysNova LUCE

The LUCE study is expected to enable future exploration missions around the Moon, by pushing the following key technologies:

- Deployment and autonomous operation of a number of small satellites in a lunar orbit either as individual elements or as part of a distributed system including localization and navigation aspects;

- Miniaturization of optical, RF, and other scientific payload instrumentations and associated technology flight demonstrations on CubeSat/nanosatellite platforms in a lunar orbit;
- Remote sensing of the lunar surface and/or in-situ measurements in the lunar environment and astronomical observations that could be made from lunar orbit and not achievable by past, current, or planned lunar missions;
- Intersatellite communication links to a larger lunar communications orbiter for relay of data back to users on Earth and for tracking, telecommand, and control;
- Technologies directly useful for future human and robotic exploration missions and in need of flight demonstration in a representative environment.

The mission concept relies on a lunar orbiter which departs from Earth and reaches an elliptical (800–8000 km) high-inclination (50°–90°) orbit where it deploys several smaller satellites (up to 24 kg) in a circular orbit around the Moon. This mother spacecraft solves most of the issues related to the deployment in lunar orbit, and it also ensures communication with Earth, acting as a relay to the small satellites (it should be noted that, according to the SysNova LUCE challenge, no direct-to-Earth communication was allowed). This concept brings several constraints on the small spacecraft, especially from the communications point of view. The mother spacecraft is only visible in certain parts of the orbit (see Fig. 1), and it constrains the communications to and from Earth as it can service only one satellite at the time in time-division multiple access. Furthermore, the mother spacecraft does not have a known schedule, so the deployed satellites should act independently and be able to fulfill their goals without counting on a connection to ground. An additional 10 days maximum communication blackout should also be considered, in case of problems onboard the mother spacecraft. One of the aims of SysNova LUCE is pushing the limits of technology, and autonomous operations will be an important technology to demonstrate for future missions.

2.2 Lunar Meteoroid Impact Observer

LUMIO is one of the four missions that were funded by ESA, and it is meant to observe, quantify, and characterize the meteoroid impacts by detecting the impact flashes on the lunar farside. This will complement the knowledge gathered by Earth-based observations of the lunar nearside, thus synthesizing global information on the lunar meteoroid environment.

The mission is designed to observe meteoroid impacts on the lunar farside for a continuous period (up to 14 consecutive days) to improve the existing statistics on meteoroids close to Earth. The Moon can be used as an impact target to measure the statistics, but Earth-based observations of lunar impact flashes are restricted to periods when the lunar nearside is illuminated between 10 and 50%. The observation on the night side of the Moon can be carried out when the illumination is less than 50%, and this can happen for half of the lunar orbit. To achieve this, it was required

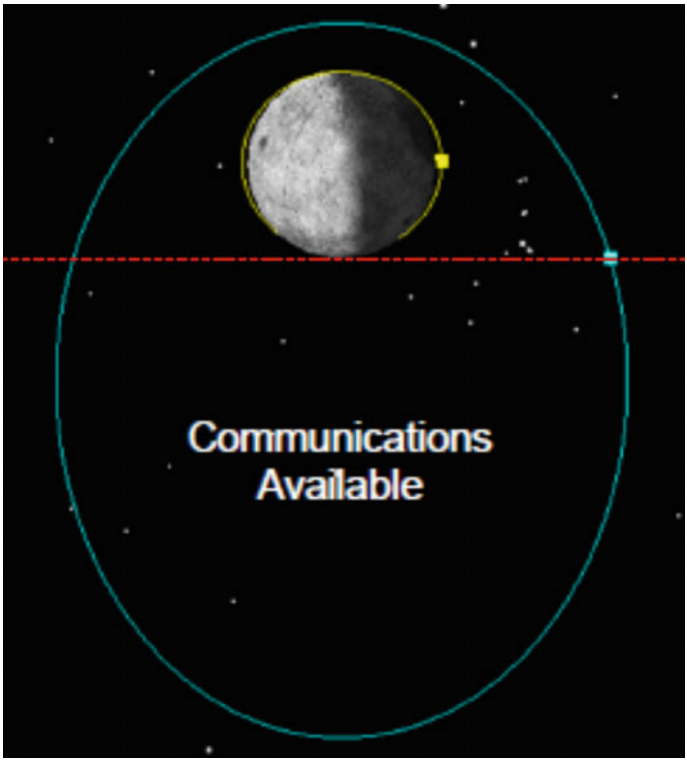

Fig. 1 Lunar orbiter communication window (see Sect. 3 for further details)

to select an orbit that would maximize the visibility on the night side of the Moon (see Fig. 2 for more details).

The mission uses a CubeSat that carries the LUMIO-Cam, an optical instrument capable of detecting light flashes in the visible spectrum. LUMIO-Cam has a 1024 $\times$ 1024 pixel CCD, 6° FOV, 127 mm focal length, and 55 mm aperture. Slight defocusing is chosen to prevent detecting false positives. Onboard data processing is implemented to minimize data downlink, while still retaining relevant scientific data. The onboard payload data processor autonomously detects flashes in the images, and only those containing events are stored.

The mission implements a sophisticated orbit design: LUMIO is placed in a halo orbit about Earth–Moon L_2 where permanent full-disk observation of the lunar farside is made. This prevents having background noise due to Earth shine and thus permits obtaining high-quality scientific products. Repetitive operations are foreseen, the orbit being in near 2:1 resonance with the Moon orbit. Innovative full-disk optical autonomous navigation is proposed, and its performance is assessed and quantified.

The spacecraft is a 12U form-factor CubeSat (see Fig. 3 for further details), with a mass of 22 kg. Novel onboard micropropulsion system for orbital control, de-

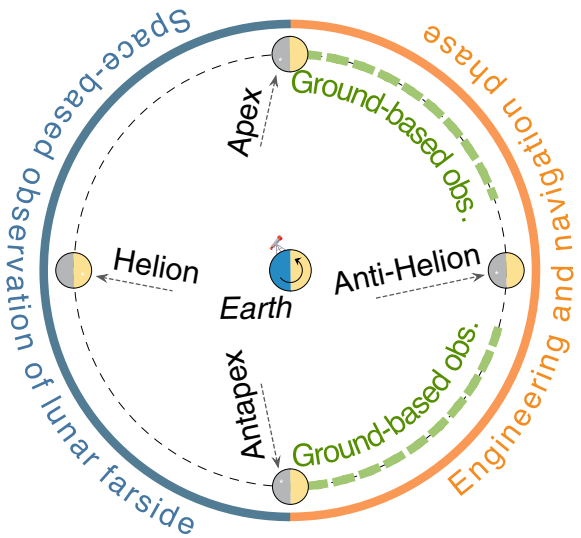

Fig. 2 Improvement in observation time of lunar farside

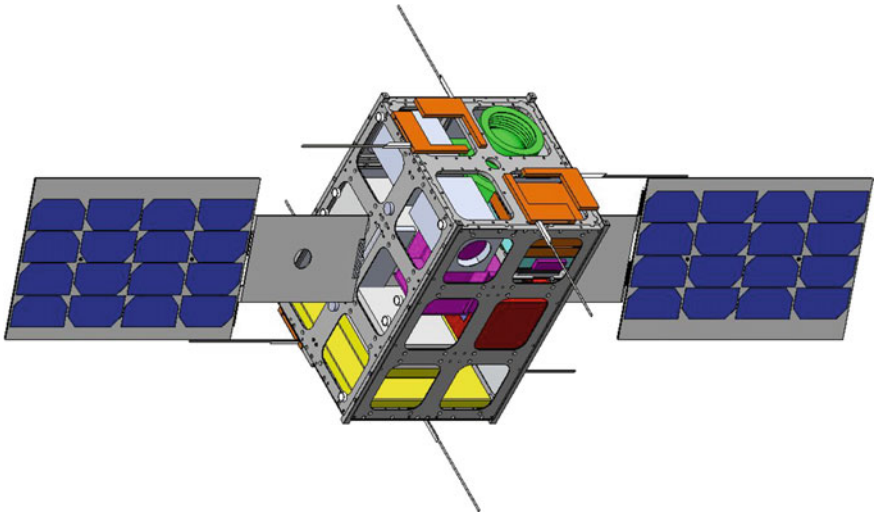

Fig. 3 LUMIO configuration

tumbling, and reaction wheel de-saturation is used. Steady solar power generation is achieved with a solar array drive assembly that also guarantees eclipse-free orbits. Accurate pointing is performed by using reaction wheels, an IMU, start trackers, and fine sun sensors. Communication with the lunar orbiter is done in the UHF band using the CCSDS Proximity-1 link [4]. A lightweight structure with radiation shielding has been considered to minimize the impact of ionizing radiation on components, allowing to reduce mission cost by relying on commercial parts whenever possible.

To make such a mission possible, a propulsion system capable of a Δv of 154 m/s (see Sect. 4.2) will be required. Several commercial units have been evaluated, deeming such system feasible, but requiring a high level of customization. The required volume for such a system has been estimated down to approximately 3U with a wet mass of 5.6 kg.

3 System Design

The LUMIO spacecraft has been designed to perform with a high level of autonomy, particularly the navigation, payload data processor, and CDHS subsystems. This choice was driven not only by the operational constraints with respect to the lunar orbiter, but also by the ambitious mission design. Additionally, a general zero-redundancy approach has been adopted for all subsystems. This is dictated by the tight mass and volume constraints and a CubeSat design-driven risk approach.

In the subsystem design, a systematic trade-off procedure has been adopted, based on subsystem-specific performance criteria, as well as standard performance, cost, and schedule criteria. Consistent design margins have been used for sizing the subsystems based on the development status. A standard 5, 10, and 20% mass margin has been applied for a fully COTS solution, a COTS solution requiring modification and a custom design, respectively.

The most important system and subsystem requirements are summarized in Table 1.

3.1 Payload

The observation of the light flashes produced by meteoroid impacts on the Moon farside is performed through the LUMIO-Cam, the main payload of the LUMIO CubeSat.

The impact flashes on the Moon can be modeled as black body emissions [5], with temperatures between 2700 and 6000 K [6], and durations greater than 30 ms [7]. The lowest impact energies correspond to apparent magnitudes higher than six as seen from Earth. These characteristics drive the payload requirements, which are listed in Table 2. The camera detection and optics are guided by requirements PLD-001 to PLD-003, while requirements PLD-004 to PLD-007 constrain the payload physical properties in terms of total mass, volume, power consumption, and storage, due to the need of compliance with low-resource CubeSat standards.

The baseline detector is the CCD201 of E2 V L3Vision^{TM}. This device is a 1024 $\times$ 1024 pixel frame transfer sensor that uses a novel output arrangement, capable of operating at an equivalent output noise of less than one electron at pixel rates of over 15 frames per second. This makes the sensor well-suited for scientific imaging where the illumination is limited, and the frame rate is high, as it is for LUMIO.

Table 1 Main system and subsystem requirements

OVRSYS-001	The mass of the spacecraft shall be no greater than 24 kg
OVRSYS-002	The spacecraft volume shall not exceed that of a 12U CubeSat
OVRSYS-003	The system shall operate in a standalone mode for a period of 10 days without any communication
PROP-001	The propulsion system shall provide a minimum $\Delta V = 154.39$ m/s for station keeping, orbital transfer, end-of-life disposal, and a minimum total impulse of 72.91 Ns for de-tumbling, and wheel desaturation maneuvers
PROP-002	The maximum thrust of the propulsion system shall be 500 mN
PROP-003	The propulsion system shall have a maximum thrusting time of 8 h per orbital transfer maneuver
ADCS-001	After the separation from the lunar orbiter, the ADCS shall de-tumble the spacecraft from tip-off rates of up to 30 deg/s in each axis
ADCS-003	The ADCS shall point with an accuracy of less than 0.1° during science and navigation phases
ADCS-005	The ADCS shall provide minimum pointing stabilization of 79.90 arcsec/s during the science phase
ADCS-006	The ADCS shall provide a maximum slew rate of 1°/s
EPS-002	The EPS shall supply 22 W average and 36 W peak power to the subsystems in parking orbit phase
EPS-004	The EPS shall supply 23 W average and 39 W peak power to the subsystems during transfer phase
EPS-006	The EPS shall supply 27 W average and 46 W peak power to the subsystems in science mode
EPS-008	The EPS shall supply 22 W average and 42 W peak power to the subsystems in navigation mode
EPS-013	The EPS shall have a mass of no more than 3 kg
COMMS-001	The spacecraft shall receive telecommands from lunar orbiter at the frequency range of 390–405 MHz
COMMS-002	The spacecraft shall send telemetry to the lunar orbiter at the frequency range of 435–450 MHz
COMMS-003	The spacecraft shall send payload data to the lunar orbiter at the frequency range of 435–450 MHz
COMMS-007	The maximum available time limit for communication between the spacecraft and the lunar orbiter shall be 1 h per day
PDLPROC-01	The payload processor shall receive and process a maximum of 15 images per seconds from payload
PDLPROC-02	The payload processor shall store a maximum of 13 MB of payload data per 29 days period to the COMMS for transmission to lunar orbiter

Table 2 LUMIO payload requirements

PLD-001	The payload shall detect flashes with energies between 10^{-6} and 10^{-1} kT TNT
PLD-002	The payload shall detect flashes in the radiation spectrum between 450 and 890 nm
PLD-003	The image integration time shall be equal or greater than 30 ms
PLD-004	The mass of the payload shall be no more than 4.5 kg
PLD-005	The maximum power consumption of the payload shall be no more than 10 W
PLD-006	The maximum size of the payload shall be 10 cm × 10 cm × 30 cm
PLD-007	The payload processor shall create less than 20 MB of science data per day

Table 3 Detector features

Parameter	Value	Parameter	Value
Image area	13.3 mm × 13.3 mm	Low noise gain	1–1000
Active pixels	1024 × 1024	Readout frequency	15 MHz
Pixel size	13.3 μm × 13.3 μm	Charge handling capacity	80 ke^-/pixel
Storage area	13.3 mm × 13.3 mm	Readout noise @1 MHz	<1e^- rms

Table 4 Optics features

FOV	Focal length (mm)	Aperture (mm)	F number
6 deg	127	55	2.3

The sensitivity of this detector extends toward the NIR region, which allows to better exploit the emission of radiation due to the impacts. The detector features are reported in Table 3.

Considering the LUMIO orbit, for which the S/C-Moon range is approximately between 35,000 and 85,000 km, a minimum payload FOV of 5.68 deg is necessary to have always the Moon full-disk view. To compensate for pointing errors and other effects, a 6 deg FOV is considered, leading to a 127 mm focal length. The LUMIO-Cam optics features are shown in Table 4.

The mechanical layout of LUMIO-Cam is shown in Fig. 4, and it includes a mechanical barrel supporting five lenses, an entrance baffle for out-of-field straylight reduction, a focal plane assembly, a proximity electronics box, and an external box for mechanical protection.

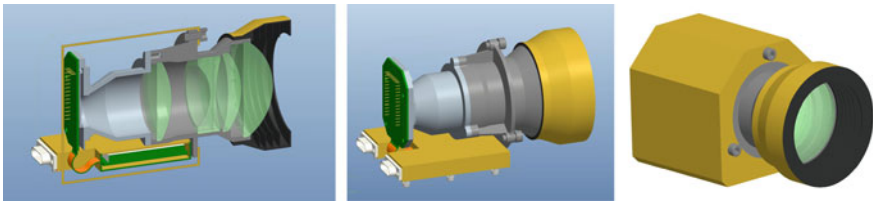

(A) Open opto-mechanical assembly (B) Closed opto-mechanical assembly (C) External box

Fig. 4 LUMIO-Cam assembly

Table 5 Payload mass and power budgets (the margin is taken to be 20%)

	Mass (kg)	Marg. mass (kg)		Power (peak) (W)	Marg. power (W)
Lenses	0.3	0.36	Detector	0.2	0.24
Barrel	0.4	0.48	TEC	2.3 (2.8)	2.76 (3.36)
Baffle	0.1	0.12	Electronics	0.5	0.6
Electronics	0.2	0.24			
Mechanical box	0.3	0.36			
Total	1.3	1.56	Total	3.0 (3.5)	3.6 (4.2)

The mass and power budgets are reported in Table 5, where a 20% margin has been considered owing to the early stage of the design. The LUMIO-Cam total margined mass is 1.56 kg, and its worst-case power consumption (margined) is 4.2 W.

A radiometric analysis employing the LUMIO-Cam properties has been performed to assess the capability of the payload to detect the phenomenon under study. The detector collects photons emitted by the impact flash, but also some undesired signals, which are considered as noise (e.g., the straylight background noise, the dark current, and the CCD's readout noise).

The SNR estimated with the radiometric analysis is always higher than 5 dB, assuring the detectability of the entire range of meteoroids impact energies.

An onboard payload data processor is required due to the high amount of data generated by the payload: for an acquisition rate of 1.8 MB images at 15 fps, the data products of the payload would be around 2.4 TB/day of science acquisitions. To reduce this amount, the OBPDP detects flashes in the images and stores only the images with scientific relevance. This leads to a reduction by a factor of about 23,000. Since not all pixels of the full frame image are scientifically relevant data, the OBPDP will also cut away everything outside an area around the flash. In this way, from 35.7 TB gathered during a LUMIO orbit period (14.7 days), just 13 MB of data needs to be stored, which is shown in Fig. 5.

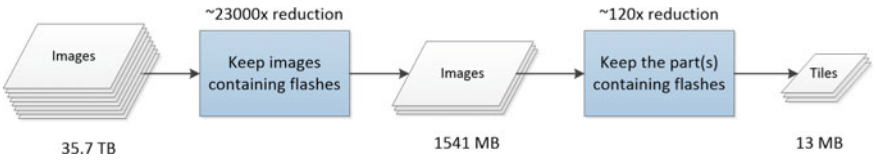

Fig. 5 Data amount reduction

3.2 Propulsion

The trade-off related to the propulsion subsystem showed that chemical propulsion is the only feasible option for the main maneuvers (orbital transfer and station keeping), since all other options pose serious risks in terms of mass, volume, and/or thrust level requirements. For the de-tumbling and de-saturation maneuvers, a clear preference should be given to a chemical or a cold-gas system. The initial proposed design is based on a partially customized version of the VACCO Hybrid ADN MiPS, including one main mono-propellant thruster (ADN green propellant) providing a thrust of 0.1 N for the main maneuvers, plus four cold-gas RCS thrusters in a "pyramid" configuration, providing a thrust of 10 mN each for the de-tumbling and de-saturation maneuvers. The preliminary design showed that the mission requirements can be accomplished with a system having a total wet mass of 5.6 kg and a total volume of 3.1U. Alternatives based on performing all required functions with the same propulsion type (mono-propellant or eventually resistojet), as well as systems based on completely European developments, are expected to be investigated and better assessed during the next mission design phases.

3.3 Attitude Determination and Control

This subsection describes the key features of the attitude determination and control system (ADCS) for LUMIO CubeSat. A trade-off analysis with different COTS components is undertaken with the aim of optimizing mass, volume, and power budgets, while adhering to the system constraints and mission requirements. The ADCS requirements are dependent upon the different phases of the mission, as shown in Table 1. These phases are (i) the de-tumbling phase where the CubeSat's angular velocity rates must be driven to rates lower than 1 deg/s from potential tip-off rates of 30°/s in each axis, (ii) an initialization phase, where the CubeSat should maneuver the solar panels toward the Sun within a time compatible with the electrical energy capability, (iii) the ADCS nominal operation phase. The ADCS nominal operation must (1) enable full-disk Moon coverage with a maximum preliminary pointing error of 0.1° which is based on simple geometric considerations about the CubeSat–Moon distance and the 3σ navigation error for the position (see Sect. 6), maximize power generation by designing an optimal attitude reference trajectory

that satisfies the Moon pointing constraints and considers the ability for the solar panels to rotate, and (3) continuously track the reference attitude in the presence of disturbances and perform slew motions within prescribed tolerances as shown in Table 1. Accurate tracking is critical for image acquisition and depends on the flash detection performance of the LUMIO camera; (4) de-saturation maneuvers will be required during the nominal operations phase of the mission to dump the momentum that is accumulated in the reaction wheels due to the solar radiation pressure torque.

The de-tumbling phase and the de-saturation maneuvers will be undertaken using RCS cold-gas thrusters of the VACCO Hybrid AND MiPS. This consists of four thrusters which can provide a torque around the roll, yaw, and pitch axis depending on which pair of thrusters is fired. The VACCO propulsion system is shown in the bottom-right corner of Fig. 8.

It can be noted that in this configuration with four thrusters, the control algorithm can be further optimized. Moreover, there are 15 possible torques (including zero torque) available at any instant in time using four thrusters, and these should be applied in such a way to de-tumble or de-saturate while minimizing an appropriate cost function such as total impulse or the total parasitic Δv resulting from the orbit-attitude coupling. The slew maneuvers and nominal operating phase are undertaken with reaction wheels. The slew motion is performed in a conventional way using a classic feedback controller such as quaternion feedback. However, for the nominal operating phase, the reference attitude is designed in a unique way, specific to this mission, to allow Moon pointing while maximizing power generation. Moreover, the reference attitude is designed to minimize the angle between the normal vector of each solar panel and the CubeSat-to-Sun vector. Minimizing this angle can be achieved by designing the reference of the attitude of LUMIO and the rotation rate of the solar panels optimally.

The resultant nominal attitude matrix ABN that connects the inertial frame N(J2000) to the body frame B is defined by assigning the first row (roll axis) to the normalized CubeSat-to-Moon pointing vector $r1 = x_M$ in the N frame, the second row (yaw axis) is then constructed by computing $r2 = x_S \times x_M$, where x_S is the normalized Sun pointing vector; the third row (pitch axis) completes the orthonormal frame. The pitch and yaw axes over 30 days starting from the injection orbit into the halo orbit are depicted in Fig. 6a. The performance metric used to define the power generation efficiency is the value of $\cos\gamma$, where γ is the Moon–CubeSat–Sun angle decomposed in terms of in-plane and out-of-plane angles. The in-plane angle, α, is the angle between the normal vector to a solar panel, which lies in the pitch-roll plane, and the projection of the unitary Sun vector projected onto that plane. The out-of-plane angle, β, defines the angle between the pitch-roll axis and the Sun vector. As the solar panels can be rotated along the yaw axis, they can be designed to track the Sun, which means following the α profile, while the β angle cannot be tracked. Therefore, the nominal attitude performance must be evaluated with respect to the angle β such that power generation efficiency is at a maximum for $\beta = 0$, i.e., when the rotation axis of the solar array is perpendicular to the Moon–CubeSat–Sun plane. The preliminary analysis for the in-plane and out-of-plane angles is represented in Fig. 6b.

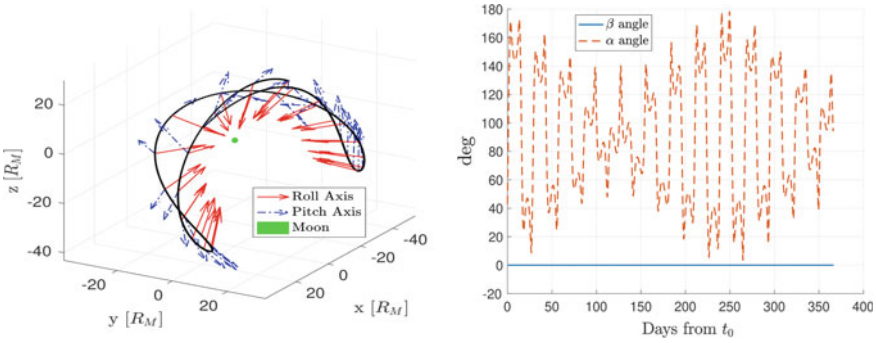

(A) Pointing for the designed attitude during the 30 days after the arrival onto the halo orbit

(B) Angles α and β during 1 year onto the halo orbit

Fig. 6 LUMIO attitude profile characteristics

In order to estimate the required control to track the aforementioned attitude profile, two simple configurations for LUMIO are considered. Initially, the center of mass is supposed to be coincident with the geometric center and the rotation axis of the solar panels aligned with the center of mass and perpendicular to the plane of the roll-pitch axes. With an assumed (worst-case) mass of 24 kg for the CubeSat, the inertia tensor for both packed and unpacked solar panels are given as:

$$J_{\text{pack}} = \begin{bmatrix} 16.66 & 0 & 0 \\ 0 & 26.00 & 0 \\ 0 & 0 & 26.66 \end{bmatrix} \times 10^{-2} [\text{kg m}^2]$$

$$J_{\text{depl}} = \begin{bmatrix} 17.41 & 0 & 0 \\ 0 & 25.66 & 0 \\ 0 & 0 & 26.25 \end{bmatrix} \times 10^{-2} [\text{kg m}^2]$$

where J_{pack} is considered during the de-tumbling phase and J_{depl} when the solar panels are deployed. The variations of the inertia due to the rotating solar panels and propulsion mass are assumed negligible at this stage.

Three reaction wheels are thought to control the CubeSat, and their rotation axes have been assumed to coincide with the principal axes of inertia. The Euler's equations for the rigid body dynamics are used to analyze the required ideal RW momentum, and the disturbance torques considered are derived from the solar radiation pressure, which has been assumed to act only on the solar panels with a total area of 0.12 m^2 and a specular reflection factor of 0.6, and the gravity gradient of the Moon. A Monte Carlo simulation is done to evaluate the contribution of the SRP in terms of distance between the CubeSat center of mass and the center of pressure of solar panels. A representative result for the required RW momentum along the halo orbit is shown in Fig. 7.

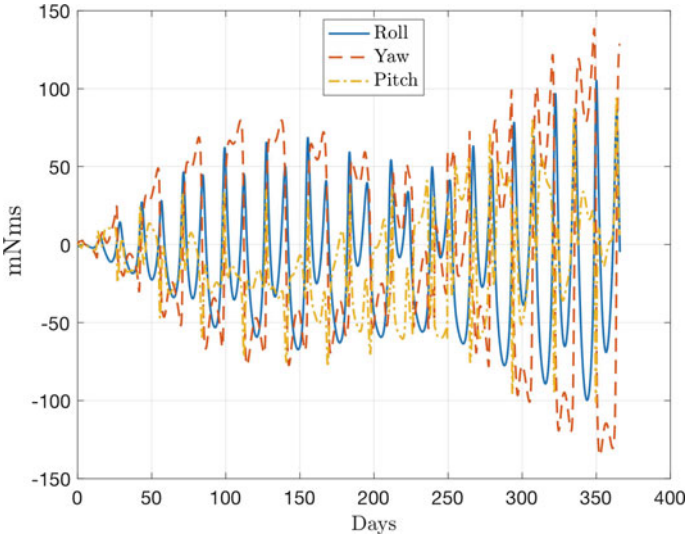

Fig. 7 Representative case of the required reaction wheel momentum to track the nominal attitude along the halo orbit

The RCS cold-gas thrusters of the VACCO Hybrid ADN MiPS are used to accomplish the off-loading maneuvers, as well as the de-tumbling phase. Off-loading requires an overall total impulse of 60 Ns, whereas de-tumbling needs 13.3 Ns.

The preliminary architecture of the ADCS subsystem for the LUMIO spacecraft is shown in Fig. 8.

The sensor suite has been chosen by selecting those with the smallest mass, volume, and power budgets given the pointing requirements and potential tip-off rates. The sensor suite comprises of a nano-SSOC-D60 Sun sensor manufactured by Solar MEMs technology (43 mm × 14 mm × 5.9 mm, 6.5 g, accuracy of 0.5° 3σ, and precision of 0.1°), two ST 400 star trackers manufactured by Hyperion Technologies and Berlin Space Technologies (53.8 × 53.8 × 90.5 mm, 280 g, accuracy of 10 arcsec 3σ in pitch and yaw, and 120 arcsec 3σ in roll axis), and an STIM 300 ultra-high performance IMU manufactured by Sensonor10 (33 cm^3, 55 g). The onboard computer is the GOMspace-Z7000, and this computer is also used for the navigation algorithm.

The actuators comprise of three Blue Canyon RWP-100 reaction wheels and the set of cold-gas RCS thrusters included in the VACCO propulsion system. The Blue Canyon RWP-100 reaction wheels are assumed to operate at a maximum of 90 mNms despite their capability of 100 mNms momentum storage. The complete ADCS system has a mass of 2 kg and a volume of 1150 cm^3.

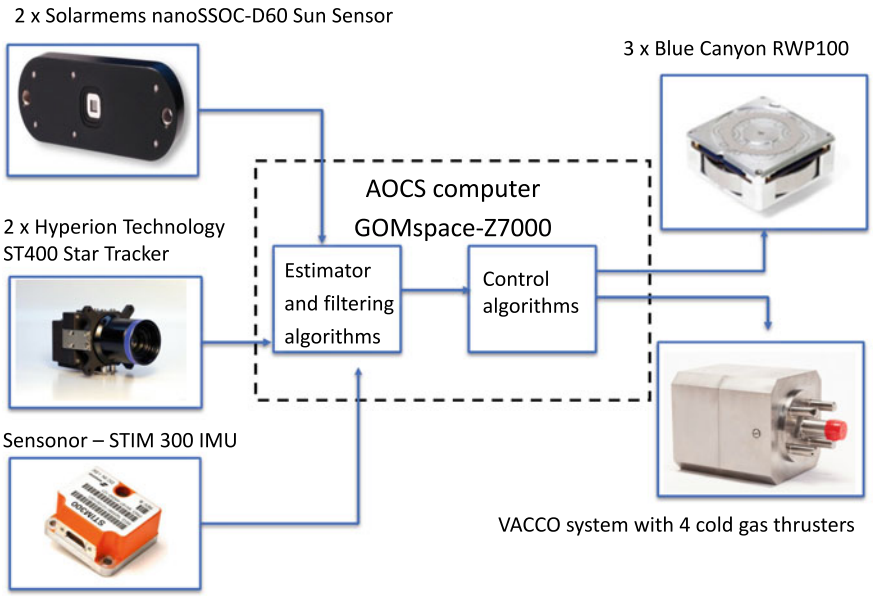

Fig. 8 LUMIO ADCS architecture

3.4 Power

For the solar array assembly, GOMSpace Nanopower MPS in its B-type configuration has been chosen, holding 16 AzurSpace 3G30C solar cell assemblies in its deployable configuration (currently under development). The size is 30 × 20 cm, with a thickness of 3.5 mm and a mass of 620 g inclusive of the solar cells. The deployable solar array is attached to a Solar Array Drive Assembly (SADA). The deployment of the solar array is achieved using a yoke which in turn is connected to the SADA inside the spacecraft. The total battery capacity is 160 Wh, achieved with two GOMSpace Nanopower BPX 80 Wh batteries.

For power conditioning and distribution, the GOMSpace Nanopower P60 unit has been selected. The interfaces between the EPS and the other subsystems are schematized in Fig. 9. The total mass of the electrical power system is estimated at 2.9 kg.

3.5 Communication

The communication subsystem is based on two UHF turnstile antennas developed by ISIS Space (one for uplink and one for downlink, considering that the typical turnstile antennas bandwidth is less than 15 MHz in the UHF band) and an RF

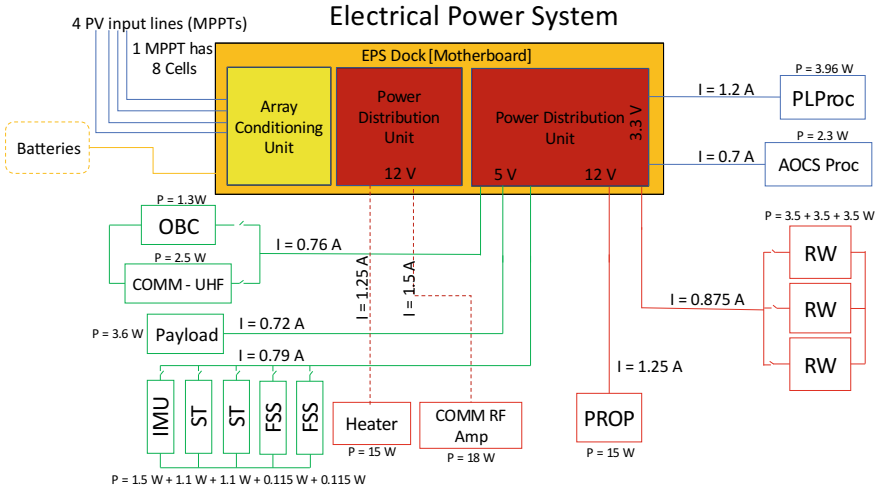

Fig. 9 Electrical interfaces between the EPS and the other subsystems

power amplifier allowing for an RF output power of 8 W, necessarily given the high transmission power required to close the link at large distances (75,000 km). The UHF transponder is based on the CCSDS Proximity-1 [4] control, with an RS442 data interface and a maximum data rate of 512 kbps.

Table 6 shows the link budgets estimated for the current configuration of the communications subsystem. In the operational phase, the PL/TM throughput is 25,919 kB for a 29-day period with 16 one-hour communication slots. This means that, when the minimum payload data requirement of 12,927 kB is met, the data budget available for telemetry is 12,992 kB. However, if this amount of TM is not required, then the payload data can be increased to downlink more frequent full-size images of the Moon.

3.6 Structure and Thermal

The main satellite structure is a COTS-based 12U CubeSat structure produced by ISIS Space. A detailed radiation analysis has been conducted in order to define the thickness of the satellite external aluminum panels for sufficient radiation shielding, taking as a reference the LUMIO operational orbit and the position of the Moon for one year. SPENVIS's solar particle model ESP-PSYCHIC (total fluence) was used to calculate the total ionizing dose (TID) and long-term single-event upsets for the operational orbit. Then, using the SHIELDOSE-2 model, the TID was plotted as a function of the thickness of aluminum shielding material of the spacecraft; see Fig. 10. Since most of the internal spacecraft components can tolerate a TID up to 20 krad, and applying a 100% margin on this value due to the large uncertainties in

Table 6 Telemetry, telecommand, and payload link budget

Link	TM return link	Payload return link	TC feeder link	Unit
Frequency	435	435	390	MHz
Modulation and coding	BPSK, rate 1/2, K = 7	BPSK, rate 1/2, K = 7	BPSK, rate 1/2, K = 7	–
Transmitter RF power	8	8	2	W
Antenna (Gr/T)	−17.4	−7.8	−17.4[a]	dB
Range	75,000	75,000	74,400	km
Data rate	1000	8000	1000	bps
Free space loss	182.7	182.7	181.7	dB
Received Eb/No	7.52	8.09	8.01	dB
Required Eb/No (BER = 10^{-6})	5	5	5	dB
Margin	2.52	3.09	3.01	dB

[a]Conservative estimate since receiver details are not known (Receiver at 60,000 km from transmitter)

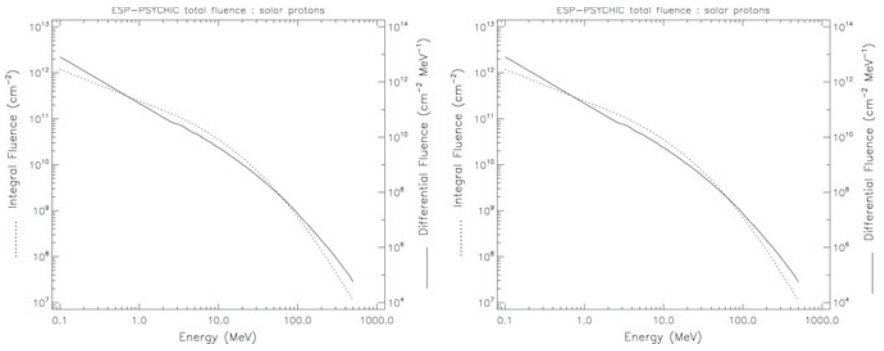

(A) Fluence spectrum (B) Total ionizing dose

Fig. 10 Radiation analysis for one-year near-Earth interplanetary circular orbit of 435,000 km radius, starting on 22 August 2023

this analysis, a thickness of 1.5 mm was selected, with additional internal shielding foreseen for particularly critical components (IMU, star trackers, SADA). The total mass of the structure designed with this criterion is 4 kg. The QuadPack deployer [8] from ISIS Space is expected to be used for deploying the CubeSat from the lunar orbiter.

A simplified steady-state single-node thermal analysis (with the main spacecraft body and the solar arrays considered as different thermally isolated bodies) has been conducted at this stage, given the still large uncertainties in the spacecraft internal and external design. Results showed that, with a combination of three different thermal

coatings (27% gold, 25% silvered teflon, 48% polished Al 6061-T6), the spacecraft temperature is expected to stay in a range from −5 to +45 °C when illuminated by the Sun. In the few eclipse periods expected during the mission, much lower temperatures down to −50 °C were estimated, which might require the use of internal heaters for further thermal protection of the most critical components.

3.7 Command and Data Handling and Onboard Payload Data Processor

The selected OBC for the LUMIO spacecraft is the AAC Microtec Sirius computer, equipped with RS-422 and RS-485 connections as well as two SpaceWire 10 Mbps links, a 32-bit fault tolerant CPU and an EDAC protected memory. A CAN bus is foreseen for the connection with the ADCS and payload dedicated computers, as well as the electrical power system; although the selected computer does not support it natively, an option is available to accommodate a CAN-compatible transceiver upon request. The connection with the communication subsystem is done with RS-422, the only type of link supported by the UHF transponder.

For the dedicated OBPDP, the GOMSpace Nanomind Z7000 processor has been selected. The OBPDP is connected to the camera through a SpaceWire interface and to the main spacecraft OBC and dedicated ADCS computer through a CAN bus. This configuration is expected to handle the required frame rate of 15 fps with a size of approximately 2 MB per frame.

3.8 Spacecraft Configuration

Figure 11 shows the current foreseen configuration for the LUMIO spacecraft, while the complete mass budget, including margins at system and subsystem level, is shown in Table 7. A total margined mass of approximately 22 kg is currently estimated for the spacecraft, well within the initial 24 kg requirement. The additional mass can be used for deviating from the zero-redundancy strategy by adding components to avoid single points of failure, for including additional propellant to extend the mission lifetime or for accommodating additional payloads to exploit secondary mission objectives.

4 Orbit

A thorough trade-off analysis has been performed to select LUMO's operational orbit. Keplerian, perturbed Keplerian, and fully three-body orbits have been considered and

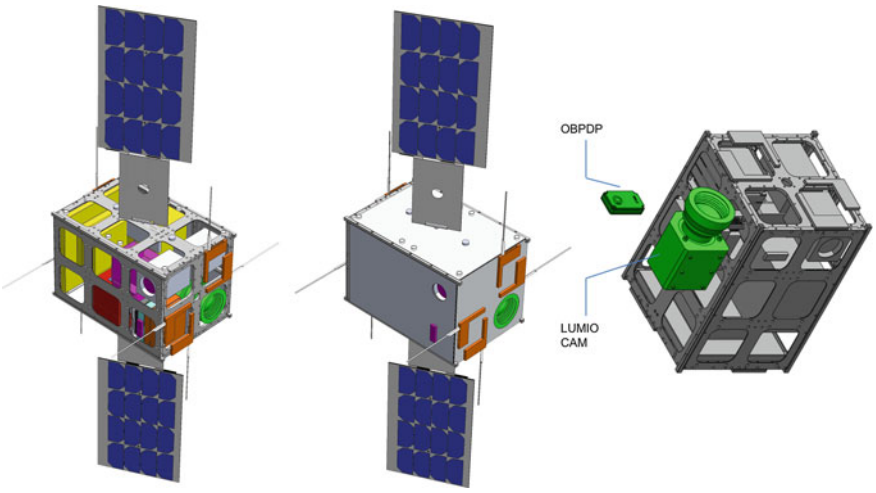

Fig. 11 Complete spacecraft without and with panels (left) and exploded view showing the LUMIO-cam (in green, right)

Table 7 LUMIO mass budget, including system and subsystem margins

Component	Mass (kg)	Design approach	Subsystem margin (%)	Mass with margin (kg)
Payload	1.3	Custom design	20	1.6
Payload Processor	0.2	Full COTS	5	0.2
Propulsion	5.6	COTS with modification	10	6.1
Communication	0.5	Custom design	20	0.6
CDHS	0.3	COTS with modification	10	0.3
ADCS	2.0	Full COTS	5	2.1
EPS	2.9	COTS with modification	10	3.1
Structure	4.0	COTS with modification	10	4.4
Thermal	0.1	COTS with modification	10	0.1
Electrical harness	0.5	COTS with modification	10	0.6
Total				19.2
System margin			10	
Total mass with system margin				21.1

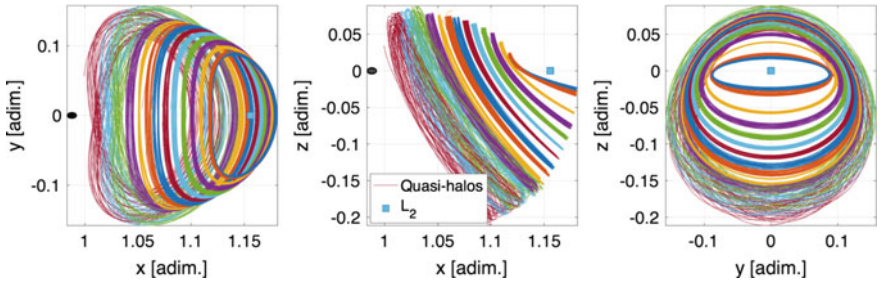

Fig. 12 Projection of Earth–Moon L_2 quasi-halos in the roto-pulsating frame

traded against a number of criteria, such as (1) the accessibility from the injection orbit, (2) the orbit lifetime and maintenance costs, and (3) the capability to cover the lunar nightside. A *preliminary trade-off* revealed that frozen orbits (perturbed Keplerian orbits) as well as halo and vertical Lyapunov orbits (three-body orbits) were good candidates, and therefore, a round of *coverage analysis* was performed. In this step, an integrated simulation accounting for models of the payload, the lunar meteoroid environment, and the orbit geometry was implemented. The analysis allowed discarding frozen orbits: because of their low altitude, these orbits can only resolve very low-energy impacts, as the detector saturates for impact energies of interest. Moreover, while both halo and vertical Lyapunov orbits met all criteria, the latter were selected as backup option because of their lower flying heritage. The L_2 halo orbit family underwent a final, *detailed trade-off*, which is described below. An exhaustive description of the orbit design for LUMIO can be found in [9].

A set of quasi-periodic halo orbits about Earth–Moon L_2 are found by employing the methodology described in [10]. Fourteen quasi-halo orbits are computed in the high-fidelity roto-pulsating restricted n-body problem and saved as SPICE kernels. The initial feeds to compute the quasi-halo samples are Earth–Moon three-body halos at 14 different Jacobi constants, ranging from $C_j = 3.04$ to $C_j = 3.1613263$. All orbits are computed starting from 2020 August 30 00:00:00.00 TDB. Although quasi-halos, shown in Fig. 12, are computed for a fixed initial epoch, the persistence of libration point orbits in the solar system ephemeris model allows wide freedom in the refinement algorithm, which also includes the mission starting at different epochs [11].

Quasi-halo orbits of Fig. 12 are all possible LUMIO operative orbits. As the orbit becomes more energetic (or as its CRTBP Jacobi constant decreases), the quasi-halo exhibits a wider range of motion both in terms of (a) Moon range and of (b) geometrical flight envelope about the corresponding CRTBP trajectory. The latter trend is disadvantageous when a hard-pointing constraint must be respected (e.g., Moon full-disk on optical instrument). On the other hand, the lunar distance places a constraint on the minimum FOV for the optical instrument on board LUMIO to be able to resolve the Moon full-disk at any location along the quasi-halo.

Table 8 LUMIO mission Δv budget

Maneuver	Cost			
	Deterministic	1σ	2σ	3σ
PCM	0	–	–	–
Injection orbit SK	–	8	8	8
SMIM	89.4	–	–	–
TCM1	–	28.6	53.0	73.1
TCM2	–	6.5	15.0	24.8
HIM	0.5	–	–	–
1-year SK	–	18.3	23.9	28.1
Disposal	3	–	–	–
Total	154.4		192.9	227.0

The transfer phase of LUMIO is designed entirely in the CRTBP. Free transport mechanisms are leveraged to reach a target halo. Specifically, intersection in the configuration space is sought between the halo stable manifolds and a selenocentric transition orbit. Since the sought intersection occurs only in configuration space, a maneuver is necessary for orbital continuity. This maneuver places the spacecraft on the stable manifold of the target halo and is thus called stable manifold injection maneuver (SMIM).

Mission Δv budgets for each maneuver and phase are reported in Table 8 with both deterministic and confidence values. The 1σ is 154.4 m/s, which is also in line with a 12U CubeSat volume and mass budgets. The choice to consider a 1σ confidence interval on stochastic maneuvers for LUMIO is motivated by the inherently higher risk of a low-cost mission.

5 Concept of Operations

Autonomous operations are the key factor behind the design of LUMIO: the lunar orbiter severely constrains the amount of information that can be sent and received, and it also does not allow to plan operations in advance. Standard navigation, based on radiometric measurements with ground, is also impossible due to the lack of direct visibility. In our case, an autonomous navigation system (described further in Sect. 6) has been designed to account for the lack of direct communication with Earth.

Besides the navigation system, the concept of operations needs to be designed taking autonomy into account and including fault detection to keep the satellite in a safe condition when an unexpected problem occurs. In this case, the satellite needs to wait for intervention from Earth, via the orbiter, to resolve the issues. This safe condition might last up to 10 days during which the satellite has to keep the battery

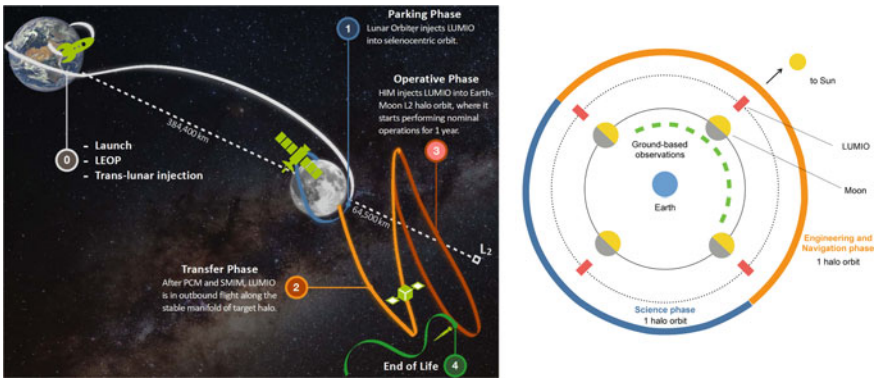

(A) Overall mission operational concept (B) Science operational concept

Fig. 13 LUMIO operational concept

charged, the onboard temperatures within margins and maintain pointing to be sure to communicate with the orbiter.

The starting point for the mission is the epoch of ejection from the lunar orbiter. The launch of the spacecraft aboard the launch vehicle and its trajectory from Earth to Moon is under the responsibility of the lunar orbiter, and it will not be described here. The mission is divided into four main phases, as also shown in Fig. 13:

- **Parking orbit**: This is the first phase of the mission, after deployment;
- **Transit phase**: During this phase, LUMIO will autonomously plan and execute a trajectory correction maneuver to reach the planned target orbit;
- **Operational Phase**: This is the nominal mission phase, when the science observations will be performed;
- **End of life**: In this phase, LUMIO will be disposed to avoid risks for future missions.

These mission phases have been defined based on the different orbits the spacecraft follows, and each phase will have drastically different conditions and requirements. Data transfer (both telemetry and scientific data) will drive an important part of the operations due to the extremely constrained available throughput. Based on the available antennas on the orbiter (limited to -7.8 dBWK^{-1} for the high gain link and -17.4 dBWK^{-1} for the low gain link), a maximum data rate of 1 and 8 kbps are possible. Table 9 shows the estimated throughput for the different mission phases and the required communication time. As shown in the table, the payload data transfer is shared with telemetry data to allow monitoring and controlling the spacecraft. It can be clearly seen that a more autonomous system would allow to relax the telemetry data downlink requirement and provide more margin to payload data transfer. The following sections will focus on the different mission phases and will provide more details on each of them.

Table 9 Calculated maximum throughputs for the different data

Phase	Communication window	Payload		Telemetry		Telecommand
		(kB)	(h)	(kB)	(h)	(kB/day)
Parking	1 h/day	–	–	46,980	1	45
Transfer	1 h/day	–	–	46,980	1	45
Operations	16 h/29 days	12,927	7.9	12,992	8.1	25
		22,103	13.7	3816	2.3	25

5.1 Parking Orbit

This phase begins just after the orbiter releases LUMIO at the desired lunar parking orbit. In this phase, the first task is to commission the subsystems that shall perform a status check for all to ensure their proper working. Preparations for the execution of the next phase are also done. It is important to stress here that the commissioning phase shall be completely independent (as opposed to most current CubeSat missions).

Once the proper working is ensured and the status of the systems is gathered, de-tumbling of LUMIO is performed to reduce the spin and stabilize it before the deployment of the solar arrays. This mode is important to start communications with the orbiter and initiate power generation. In case of a commissioning failure, LUMIO will have to seek help from Earth. Given the proposed injection orbit stability, minimal orbital corrections will be required for station keeping for approximately 14 days: this will guarantee enough time (considering a maximum of 10 days communication blackout included in the original SysNova LUCE challenge) for proper control from ground, without impacting significantly the available propellant onboard.

After full deployment, LUMIO enters the cruise mode where the attitude control and navigation image acquisition will be done. For every revolution around the Moon, a station-keeping maneuver is performed to maintain the desired position and velocity.

5.2 Transfer Phase

Transfer trajectory optimization has been done for transfers from the parking orbit to the quasi-halo orbit about L_2 considering the multibody dynamics and minimization of propellant mass and time of flight. The analysis resulting from trajectory optimization yielded parameters that satisfy the mission requirements.

The transfer phase consists of four modes:

- **Transfer Maneuver Mode**: It contains three tasks, the manifold injection maneuver, trajectory correction maneuver (2x), and halo injection maneuver. The first task is to inject LUMIO in a stable manifold to set it on course, the second one is

to correct the trajectory and reduce the deviation with the guidance, and the last one is to insert LUMIO into a halo orbit.
- **Transfer Cruise Mode**: LUMIO cruises between every thrusting maneuver.
- **Data Transmission**: LUMIO communicates with the lunar orbiter and transmits the data.
- **Desaturation**: At the end of the phase, the reaction wheels are desaturated. Navigation acquisition, orbit, and attitude determination are done to ensure the correct positioning of LUMIO. This is necessary to commence the operational phase of the mission.

The navigation system is responsible for determining the proper time for the trajectory correction maneuvers to reach the desired science orbit: the main rationale for this selection is the possible absence of contacts to ground control (always via the lunar orbiter) just before the trajectory correction maneuver.

5.3 Operational Phase

The most important phase of the mission is the operational phase. The duration of this phase is one year, and it has two main modes: science mode and navigation and engineering mode. The two modes occur within one synodic period (29.53 days) and are equally split with 14.765 days each. The operations are duty cycled, and in one year, we have 12.3 cycles of science and navigation and engineering modes alternating between each other. This is shown clearly in Fig. 13b. Before entering one of these modes, there is a need to perform a commissioning of the payload data processor for science operations and payload instrument calibration to ensure its functionality and its readiness for meteoroid impacts observation.

5.4 End-of-Life Disposal Phase

At the end of the operational phase, LUMIO needs to be de-commissioned and disposed safely. The first step is to transmit the last pieces of data to the orbiter. All correction maneuvers are halted, and the batteries are discharged until a small fraction of the energy required for the EOL disposal maneuver. Finally, the propulsion system thrusts to execute the EOL disposal maneuver. Since we are in the early stages of mission development, the requirements regarding the environmental safety are still in development. The current strategy is to leave the Earth–Moon system as there would be a significant risk to impact future missions.

Table 10 LUMIO navigation requirements

ID	Requirement
NAV.001	The system shall perform autonomous onboard navigation
NAV.002	The navigation system shall determine the components of the satellite position vector within a 30 km accuracy during engineering operations phase
NAV.003	The navigation system shall determine the components of the satellite velocity vector within a 0.5 m/s accuracy during engineering operations phase
NAV.004	The navigation system shall determine the components of the satellite position vector within a 30 km accuracy, 24 h before the station-keeping maneuver execution in any phase
NAV.005	The navigation system shall determine the components of the satellite velocity vector within a 0.3 m/s accuracy, 24 h before the station-keeping maneuver execution in any phase
NAV.006	The state update frequency shall be equal or lower than 1 update/min

6 Autonomous Navigation

One of the enabling technologies for LUMIO and other missions is autonomous navigation. Traditionally, spacecraft orbit determination is performed via radiometric tracking, but this implies the costs related to the ground segment, which do not scale down with mission size as other costs. Therefore, autonomous navigation is required for small spacecraft, and demonstrating this capability is a major objective of LUMIO [12]. Autonomous navigation will also allow to drastically reduce the operational cost and complexity of this mission, as was described in Sect. 5.

6.1 LUMIO Navigation Requirements

The navigation subsystem requirements for the LUMIO mission are listed in Table 10. The requirement NAV.001 comes from the ESA SysNova statement of work which demands an autonomous onboard navigation system to be tested on a CubeSat. The accuracy needed for the position and velocity estimations as function of the mission phase, due to payload, mission analysis, and S/K constraints, is stated in the requirements NAV.002-005. Lastly, NAV.006 imposes a higher bound for the state update frequency for navigation purposes.

6.2 Navigation Techniques Trade-off

Table 11 trades-off navigation techniques about autonomy, accuracy and sensor technology, for LUMIO. The demand of autonomous navigation excludes the Earth-

Table 11 LUMIO navigation techniques trade-off

	Autonomy	Accuracy	Sensor
Radiometric Tracking	NO	Order of meters	OK
Pulsar Navigation	OK	Order of km	NO
Celestial Triangulation	OK	Order of 10^3 km	OK
Horizon-Based Navigation	OK	Order of 10^2 km	OK

OK	Compliant	~	Adaptable	NO	Unacceptable

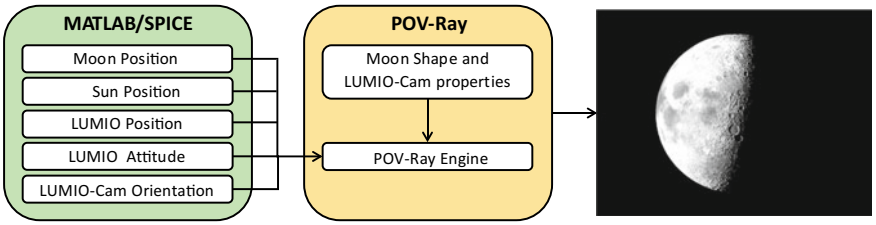

Fig. 14 Image generation process. The LUMIO–Moon–Sun geometry is defined in SPICE kernels, which is used in conjunction with POV-Ray to render Moon images

based radiometric navigation for LUMIO. Autonomous navigation options are then the X-ray pulsar navigation (X-NAV) [13], the celestial triangulation [14], and the horizon-based navigation [15]. The X-NAV, which performs spacecraft positioning by processing pulsar signals, is affected by sensor miniaturization difficulties. The celestial triangulation technique estimates a spacecraft position by triangulating with some observed celestial objects with known ephemeris, but is not compliant with LUMIO navigation requirements. The horizon-based navigation directly uses the Moon full-disk images to estimate the spacecraft position. This is achieved by detecting the Moon full-disk in an image and linking the Moon apparent size with the real one to estimate the relative distance. The full position vector can be estimated provided that Moon ephemeris and LUMIO attitude are known. The horizon-based navigation is the baseline option for LUMIO.

6.3 Simulator

The images acquired by the LUMIO-Cam are simulated employing POV-Ray, a rendering software which generates synthetic Moon images as a function of camera position, orientation, and properties. Figure 14 shows the simulator architecture. In the MATLAB working environment, the SPICE toolkit is employed to set the LUMIO–Moon–Sun orbital geometry and the LUMIO attitude. This data is sent to POV-Ray, where properties belonging to the LUMIO-Cam are present, and a Moon image can be rendered.

Fig. 15 Lunar images processing: (1) image acquisition; (2) edge finding; (3) full-disk estimation

6.4 Horizon-Based Navigation

The horizon-based optical navigation [15] employs the full-disk view of a spherical or ellipsoidal object to estimate the relative camera-to-object position vector. This is achieved by detecting the object full-disk in an image and linking the apparent object size in pixels with the real one. The image processing steps are shown in Fig. 15. Once a Moon image is acquired (1), its edge is detected (2) through image processing algorithms (e.g., Canny edge detection [16]), and an ellipse is fitted to the observed horizon points (3). The ellipse is an estimation of the object full-disk and feeds the horizon-based optical navigation algorithm.

6.5 Navigation Outputs

The images simulator described in Sect. 6.3 has been employed to generate 100 images during the LUMIO halo orbits to test the horizon-based optical navigation shown in Sect. 6.4. The optical navigation algorithm reports a total position error (norm of position error vector) always below 265 km, with 68% of the outcomes bounded in 85 km total error. An extended Kalman filter for navigation has been implemented, and a margin of 37.35% has been applied to the maximum total error as input to the filter. This is required for the novelty of the navigation algorithm. The navigation filter must consider the requirements in Table 10, and the filter requirements to satisfy, tunings, and performances are shown in Fig. 16. The halo periods are delimited by the dashed vertical lines. The station-keeping planning in terms of maneuvers execution and cutoff times for accurate navigation is shown in Fig. 16a, where three station-keeping maneuvers are planned for each engineering orbit and none is present in the scientific orbit. Accurate navigation is required 24 h in advance of the maneuvers (cutoff time). To comply with this, the acquisition frequency has been fine-tuned employing three different values, which are 16.7 MHz (high frequency—HF), 1.67 MHz (medium frequency—MF), and 0.277 MHz (low frequency—LF), and their employment is shown in Fig. 16b. The high acquisition frequency is used before the cutoff time for SK, while measurements are acquired with the medium frequency during nominal operations in the engineering orbit. For

(A) Station-keeping maneuvers planning and execution times. Three maneuve rs are commanded each engineering orbit while none is present in the scientific orbit. The cut-off time for accurate navigation is 24 hours in advance of the maneuvers execution.

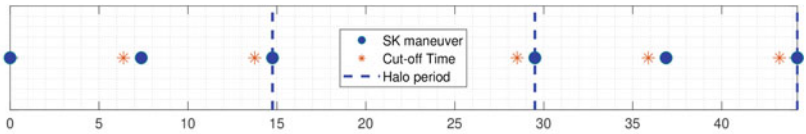

(B) Measurements acquisition frequency tuning. During the engineering orbit, the HF is employed at the cut-off time for SK maneuvers, otherwise the MF. During the scientific orbit, measurements for navigation are acquired with the LF, except when higher frequencies are required for station keeping duties.

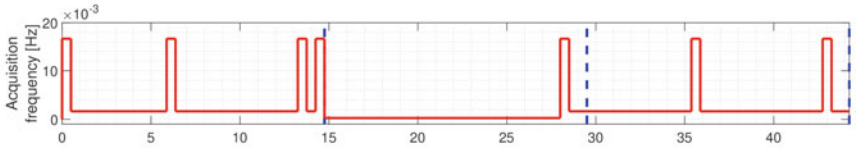

(C) Outputs of navigation filter in terms of position 3σ covariance bounds. The spacecraft position is always determined within 30 km during the engineering orbit and 50 km during the scientific orbit.

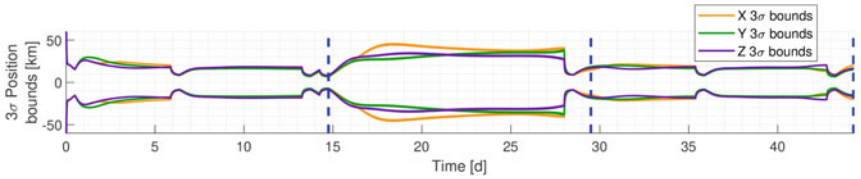

Fig. 16 **a** Station-keeping planning, **b** acquisition frequencies, and **c** navigation filter outputs in terms of position components for LUMIO

the scientific orbit, measurements are acquired with the low frequency to relax the processing required for navigation and dedicate it to scientific images processing. The 3σ position bounds for each component are shown in Fig. 16c. The outputs of the navigation filter for LUMIO are compliant with requirements in Table 10.

7 Delta Design and Future Work

Having won the LUCE SysNova competition granted LUMIO an independent assessment by the CDF team at ESA. The focus of this exercise was to improve the baseline design in identifying weak areas in a collaborative concurrent working approach. Particular emphasis was put on

- Mission and system requirements definition/analysis
- Mission, system, and subsystem-level design trade-offs
- Conceptual design of the CubeSat and its predicted performance
- Programmatic aspects (including cost, schedule, risk)
- Identifying critical issues to be further addressed

The review was carried out in five sessions in February 2018 by an integrated team of ESA specialists from various ESA sites. A review report [17] was produced, which covers the domain-specific review of the consortiums documents and identifies the problems/queries associated with the proposed design as well as proposing alternative solutions. Below, the *main conclusions* relating to the review and further actions identified are briefly listed. The reader may refer to [17] for detailed information.

7.1 Payload Design

To increase the payload performance a second channel (NIR) was suggested to be added, but it would require more power than the available one to maintain the temperature in the operational range. A second visible imager has instead been added with a dichroic crystal to split the signal into two separate visible ranges.

To decrease the risk of straylight and decrease the sun exclusion angle, the baffle was increased in size by moving the payload deeper in the satellite which allowed a longer baffle to be accommodated. A full straylight analysis and baffle optimization will be made.

Other open points on payload were identified which will be investigated as part of a next phase, namely

- Further investigation of the calibration is needed
- A dichroic could be added to the payload.

7.2 Mission Design

The focus was on possible launch opportunities. For this, the Lunar Pathfinder mission was baselined. This baseline provided the starting assumption for the release orbit (iterated with the Lunar Pathfinder team) and resulting Δv requirements to transfer to and operate in Earth–Moon L_2 halo orbit. The LUMIO mission was found to be compatible with the Lunar Pathfinder mission constraints.

As part of the CDF study, a navigation strategy was further elaborated and an update to the navigation performance requirements was given. In future phases of the project, a more detailed look in the navigation concept and performance will be given.

7.3 Platform Design

Multiple design changes were made on the platform

- The increase of the Δv budget required a change in the propulsion system baseline. Therefore, a liquid propulsion system was chosen. The proposed baseline employs two non-European thrusters each with four nozzles removing the need of a separate attitude control system.
- The total data generated has increased due to the extra payload on board. To transfer all this data, the communication system has changed to a direct-to-Earth link. This direct-to-Earth communication link also provides the possibility to monitor any critical orbital maneuvers.
- The increase in data generation rate from the payload resulted in the need for a more performant data handling system, in particular in the onboard image processing capabilities.
- The power budget increased, and therefore, the number of solar panels was increased accordingly, remaining compatible in stowed configuration with the CubeSat deployer constraints.
- Multiple options have been investigated in case some constraints come up in a later phase of the design.

7.4 Programmatic

A Proto-Flight Model development approach was selected. The TRL levels of all mission elements were assessed, and the main development items are identified. The development plan was looked into, and it ensured it is in line with the Lunar Pathfinder. A preliminary ROM cost was estimated for LUMIO considering the model philosophy.

8 Conclusions

In this chapter, we described the SysNova LUCE challenge and presented in details LUMIO, one of the four missions that were part of the challenge. LUMIO observes meteoroid impacts on the lunar farside in order to study the characteristics of meteoroids and to improve existing meteoroid models. The mission utilizes a 12U form-factor CubeSat which carries the LUMIO-Cam, an optical instrument capable of detecting light flashes in the visible spectrum to continuously monitor and process the data. The mission implements a novel orbit design and latest CubeSat technologies to serve as a pioneer in demonstrating how CubeSats can become a viable tool for deep space science and exploration. In this chapter, we focused on the autonomous operations strategy that is required to guarantee the success of the mission, also looking into autonomous navigation. We showed how LUMIO will be capable of estimating its position and calculating navigation information without help from ground. LUMIO, as presented in the chapter, will not rely on common navigation and control strategies, and this will make it a precursor for future autonomous missions toward

planetary bodies. In this chapter, we also showed an independent verification of the design carried out by the ESA CDF team that confirmed the overall design and suggested improvements to the mission as future work.

Acknowledgements This work has been funded through the ESA GSP program, Contract No. 4000120225/17/NL/GLC/as, as part of the SysNova LUCE challenge. LUMIO won ex aequo the challenge and was awarded a session in the ESA CDF to verify and refine the mission concept. We are thankful to ESA for the support received and in particular to its CDF team for the delta design conducted.

References

1. Speretta, S., Topputo, F., Biggs, J., Di Lizia, P., Massari, M., Mani, K., et al. (2018) LUMIO: achieving autonomous operations for Lunar exploration with a CubeSat. In *2018 SpaceOps Conference* (AIAA 2018-2599).
2. Walker, R., Vennekens, J., Fisackerly, R., Carpenter, J., & Carnelli, I. (30/05/2017). LUnar CubeSats for Exploration (LUCE) mission concept studies. In 6th Interplanetary CubeSat Workshop, Cambridge, UK.
3. Walker, R., Koschny, D., Bramanti, C., & Carnelli, I. (30/05/2017). ESA CDF Study Team, Miniaturised Asteroid Remote Geophysical Observer (M-ARGO): A stand-alone deep space CubeSat system for low-cost science and exploration missions. In 6th Interplanetary CubeSat Workshop, Cambridge, UK.
4. Proximity-1 Space Link Protocol—Rationale, Architecture, And Scenarios, CCSDS Green Book, CCSDS 210.0-G-2
5. Suggs, R. M., Moser, D. E., Cooke, W. J., & Suggs, R. J. (2014). The flux of kilogram-sized meteoroids from lunar impact monitoring. *Icarus, 238*(Supplement C), 23–36.
6. Oberst, J., et al. (2012). The present-day flux of large meteoroids on the lunar surface—A synthesis of models and observational techniques. *Planetary and Space Science, 74,* 179–193.
7. Bouley, S., et al. (2012). Power and duration of impact flashes on the moon: Implication for the cause of radiation. *Icarus, 218*(1), 115–124.
8. Rotteveel, J., & Bonnema, A. (2017). Launch services 101, managing a 101 CubeSat launch manifest on PSLV-C37. In *2017 Small Sats Conference*, Logan, US.
9. Cipriano, D. A., Tos, D., & Topputo, F. Orbit Design for LUMIO: The lunar meteoroid impacts observer. In *Frontiers in Astronomy and Space Sciences*, to appear https://doi.org/10.3389/fspas.2018.00029.
10. Dei Tos, D. A., & Topputo, F. (2017). On the advantages of exploiting the hierarchical structure of astrodynamical models. *Acta Astronautica*, *136*, 236–247.
11. Dei Tos, D. A., & Topputo, F. (2017). Trajectory refinement of three-body orbits in the real solar system model. *Advances of Space Research, 59*(8), 2117–2132.
12. Franzese, V., Lizia, P. D., & Topputo, F. (2018–1977) Autonomous optical navigation for LUMIO mission. In *2018 Space Flight Mechanics Meeting, AIAA SciTech Forum* (AIAA 2018–1977) https://doi.org/10.2514/6.2018-1977.
13. Sheikh, S. I., et al. (2006). Spacecraft navigation using x-ray pulsars. *Journal of Guidance, Control and Dynamics, 29*(1), 49–63. https://doi.org/10.2514/1.13331.
14. Mortari, D., & Conway, D. (2017). Single-point position estimation in interplanetary trajectories using star trackers. *Celestial Mechanics & Dynamical Astronomy, 128*(1), 115–130. https://doi.org/10.1007/s10569-016-9738-4.
15. Christian J. A., & Robinson S. B. (2016). Noniterative horizon-based optical navigation by cholesky factorization. *Journal of Guidance, Control, and Dynamics*, *39*(12), 2757–2765. https://doi.org/10.2514/1.G000539.

16. Canny, J. (1986). A computational approach to edge detection. *IEEE Transactions on Pattern Analysis and Machine Intelligence*, *PAMI-8*(6), 679–698. https://doi.org/10.1109/TPAMI.1986.4767851.
17. CDF Study Report: LUMIO—Review of SysNova Award LUMIO Study, ESA Report CDF-R-36, February 2018.